FINAL TECHNICAL REPORT
for
AWARD N00014-92-J-1049
October 1, 1991 - September 30, 1992

Title: "Isolation and Analysis of Key Components of Seafloor Relief"

P. I.: Dennis E. Hayes

Background: We are continuing to investigate several hypotheses regarding the processes that are responsible for forming the various components of seafloor relief and the composite seafloor roughness. We have put forward the hypothesis that the composite seafloor relief can be meaningfully divided into three or more distinctive spatial wavebands each of which can be related to different physical processes. Our goal is to understand the operative geological processes well enough to be able to better predict the complete seafloor/basement roughness characteristics where it has not been measured and for regions where it is difficult or impossible to measure accurately (e.g., buried basement relief).

Results: Regarding the hypothesis that there is a recognizable, unique spatial wave band that defines the nature of the roughness dependence on spreading rate, we have examined world-wide data from 17 high-resolution multibeam cruises. These data were selected because they are near flow-line parallel tracks and are in regions where the spreading rates can be reliably determined (see Fig.1A). All the data were filtered uniformly to retain only the relief features with spatial wavelengths (λ) of less than 25 km. The results of the RMS roughness values plotted against constant spreading rate episodes (over a large range of spreading rates) are shown in Fig. 1B. An approximately linear dependence of RMS roughness exists but there is clearly an associated high variance, especially for low spreading rates.

In order to expand the data base, we investigated the plausibility of combining closely sampled, high-resolution, bathymetric profiles with widely sampled, lower-resolution, profiles. By decimating high resolution profiles to simulate lower resolution profiles, we determined that the RMS values changed little, being reduced slightly and approximately uniformly (see Fig. 2). This then allowed us to combine data from both high and low resolution systems to create a significantly larger data base for examining RMS roughness vs. spreading rate dependence on a more comprehensive, global scale. The results from ~40 cruises, comprised of 343 segment values, are summarized in Figs.3A and 3B and the data are identified by ocean region. Our linear regression results and the inverse square-root relationship derived by Malinverno (1991) are both shown.

We conclude the following: the RMS roughness is approximately linearly dependent on spreading rate over half-spreading rates of 1.5 cm/yr to 8 cm/yr with a slope of about ~23 m/cm yr and an intercept of 200 m. For half-spreading rates below 1.5 cm/yr, the data scatter considerably though their mean values are consistent with the above relationship. Data from the Indian Ocean appear to cluster uniformly below the overall population trend and warrants further investigtion.

We have also verified that the process of asymmetric seafloor generation results in measurable differences in small scale ($\lambda < 25$ km) roughness (see also Hayes and Kane, 1991a). The generalized roughness-spreading rate relationship noted above predicts this result, given the measurable contrasts in spreading rates that serve to define asymmetric spreading. The additional data we have examined show, however, that there are occasional exceptions to this general relationship, most notably at low spreading rates.

In the process of analyzing the filtered RMS roughness data we have considered the sensitivity of the results as a function of the short wavelength cut-off frequency chosen. The results representing minimum variance correspond to cut-off frequencies of about 25-30 km and coincidentally represent the approximate spatial frequency at which seafloor roughness power spectra show a conspicuous knee -- at higher spatial frequencies the relief components exhibit a fractal relationship. We do not yet know the physical significance of the ~25 km value, but virtually all abyssal hill relief, which is thought to be formed at or within a few kilometers of the ridge axis, is included in the $\lambda < 25$ km band.

As a complement to the small scale roughness studies we have also retained and analyzed the data describing the relief characteristics in the spatial wave band between 25 km $> \lambda >$ 500 km (peak-to-peak amplitudes are typically 500-600 m, see Fig. 4A-B). The degree of cross-axis correlation of these features should provide a method by which to determine the likelihood that such features were formed on-axis and subsequently were rafted to opposite ridge flanks, or that such features were formed off-axis, independent from the spreading-crustal accretionary processes.

We have examined the residual roughness signal of intermediate wave lengths to look for a spreading rate dependence for these components as well. There is some suggestion that RMS roughness falls off with increasing spreading rate similar to the short wavelength RMS roughness see Fig. 3C), but there is greater scatter in data and it is clear that the inclusion of the intermediate wavelengths tends to obscure RMS roughness vs. spreading rate dependence relationship.

We have looked at quantitative measures of correlation of intermediate wavelength signals both along-strike (parallel to the ridge axis) and across-strike (parallel to flow-lines). The data from the North Atlantic between the Hayes and Kane fracture zones

is especially well suited for our analysis. In this area intermediate wavelength features often correlate over along-strike distances of ~50 km and for crust generated over time periods of roughly 10-20 m.y. (see Figs. 4A-C). In contrast, some episodes of crustal generation appear to exhibit little or no along-strike correlation of intermediate wavelength features. Similarly, across-strike correlations range from strongly positive to none and occasionally strongly negative correlations are found (see Figs. 4A-B, 4D). All these phenomena are recording the **integrated, long-term temporal variations** in the extent of near-axis magmatic activity, coupled with the spatial boundaries, and their adjustments with time, that define ridge segments. Episodes of contrasting high and low intermediate wavelength roughnesses are testimony to the important, pulsating nature and along-axis variability in magmatic activity.

We are just now testing the hypothesis that zones of high amplitude intermediate wavelength relief have associated short wavelength characteristics that differ, depending on whether or not the intermediate wavelength features themselves were formed on-axis or off-axis.

The total 3-D form of seafloor relief that results from the spreading process at the MOR is the result of the integration of the effects of small-scale along-axis variations (widely documented for selected areas; e.g., Grindlay et al., 1991; Macdonald et al., 1988), across-axis variations (e.g., Hayes and Kane, 1991b), temporal variations (e.g., Fox et al., 1991) and systematic regional variations (e.g., Hayes, 1988). Our goal in this study has been to analyze the differentiated portions of this composite relief signal so as to enhance the probability of understanding the mechanisms responsible for each of the main components and hence a holistic understanding of the "composite process" and an improved capability for predicting seafloor roughness.

Our studies relate directly to the Navy's stated interest in knowing how the morphology of the seafloor is created through time (temporal variability) and modified with time (evolution and aging), and in variations in space. These factors are crucial in evaluating the predictability of oceanic morphology, understanding the suite of processes responsible for its formation, and in defining the scale and limits of seafloor roughness (and hence acoustic) provinces and geological provinces. This work is continuing under award N00014-89-J-11589.

References

Fox, P. J., Grindlay, N.R., and K. C. Macdonald, 1991, The Mid-Atlantic Ridge (31°S-34°30'S): Temporal and spatial variations of accretionary processes, Marine Geophys. Res., 13: 1-20.

Grindlay, N. R., Fox, P. J., and Macdonald, K. C., 1991, Second-order ridge axis discontinuities in the South Atlantic: Morphology, Structure, and Evolution, Marine Geophys. Res., 13: 21-49.

Hayes, D. E., 1988, Age-depth relationships and depth anomalies in the Southeast Indian Ocean and South Atlantic Ocean, J. Geophys. Res., 93, No. B4: 2937-2954.

Hayes, D. E., and K. Kane, 1991a, The dependence of seafloor roughness on spreading rate, Geophys. Res. Lett., 18, #8: 1425-1428.

Hayes, D. E., and K. Kane, 1991b, A quantitative look at discrete components of seafloor relief (abs.), EOS, 72, #44: 454.

Macdonald, K. C., Fox, P. J., Perram, L. J., Eisen, M. F., Haymon, R. M., Miller, S. P., Carbotte, S. M., Cormier, M.-H., and A. N. Shor, 1988, A new view of the Mid-Ocean Ridge from the behavior of ridge-axis discontinuities, Nature, 335: 217-225.

Malinverno, A., 1991, Inverse square-root dependence of mid-ocean ridge flank roughness on spreading rate, Nature, 352: 58-60.

Figure Captions

Figure 1 A) SeaBeam track locations roughly parallel to flowlines.
B) RMS roughness results from SeaBeam tracks shown in 1A.

Figure 2 A) Original and decimated bathymetric signal from C2711 (South Atlantic; East Flank).
B) Effect of sample decimation on calculated RMS roughnesses.

Figure 3 A) SeaBeam and other bathymetry tracks roughly parallel to flowlines.
B) RMS roughness results with linear regression (dashed line) and with Malinverno (1991) relationship (solid line) derived from other data.
C) RMS roughness vs. spreading rate for intermediate ($25\ km < \lambda < 500\ km$) wavelengths.

Figure 4 A) N. Atlantic tracks (Kane - Hayes FZ region)
B) Exemplary profiles for Intermediate (λ_I) only
C) Along-axis λ_I correlations
D) Across-axis λ_I correlations

SEABEAM CRUISES

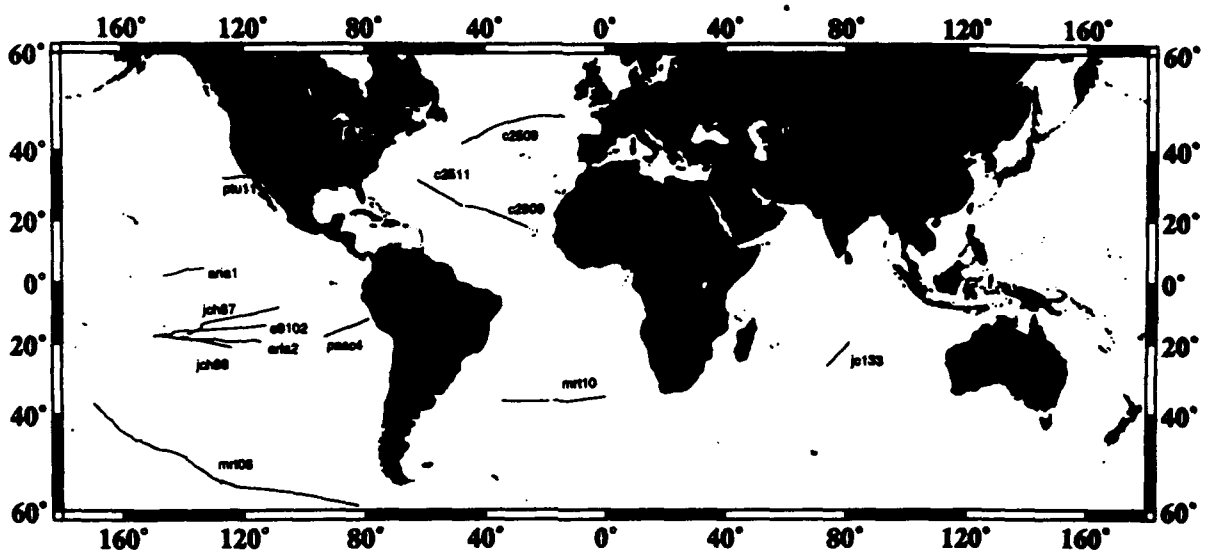

Figure 1A

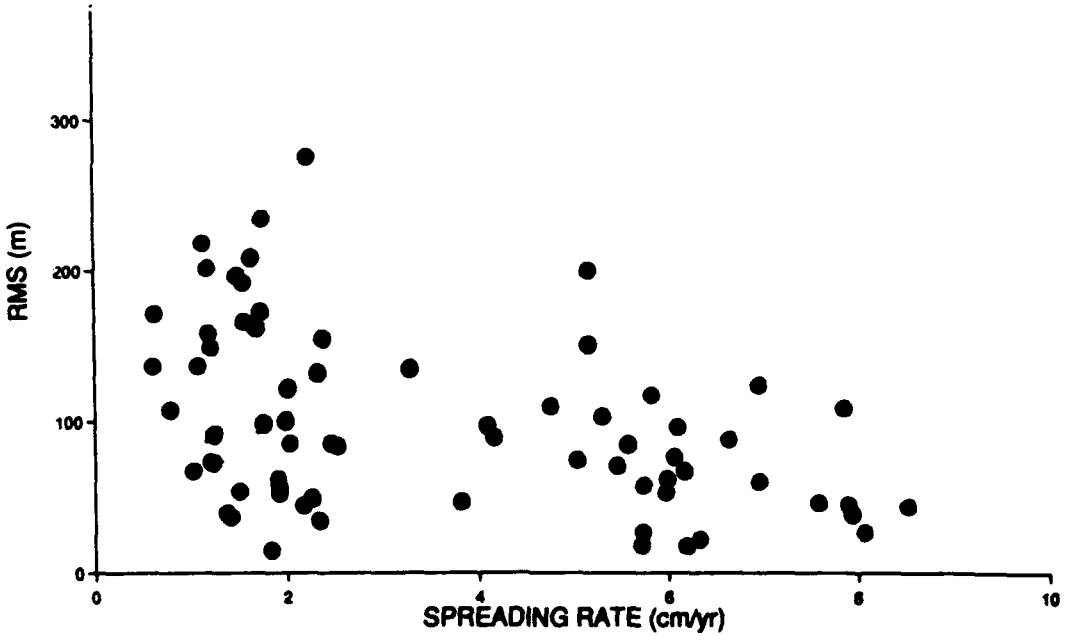

Figure 1B

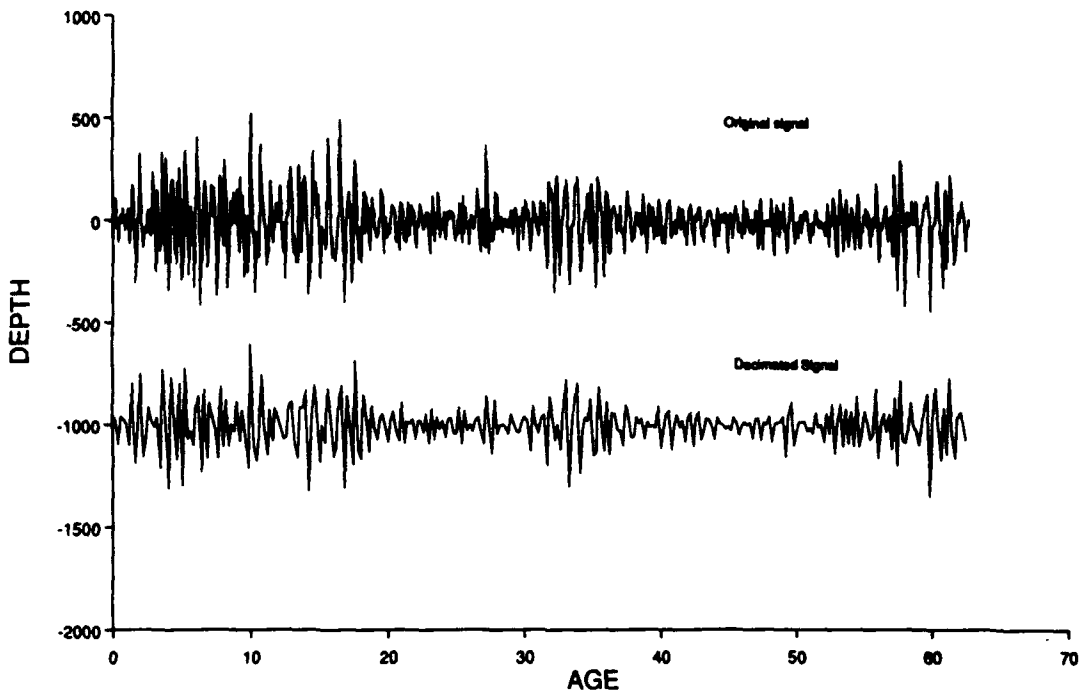

Figure 2A

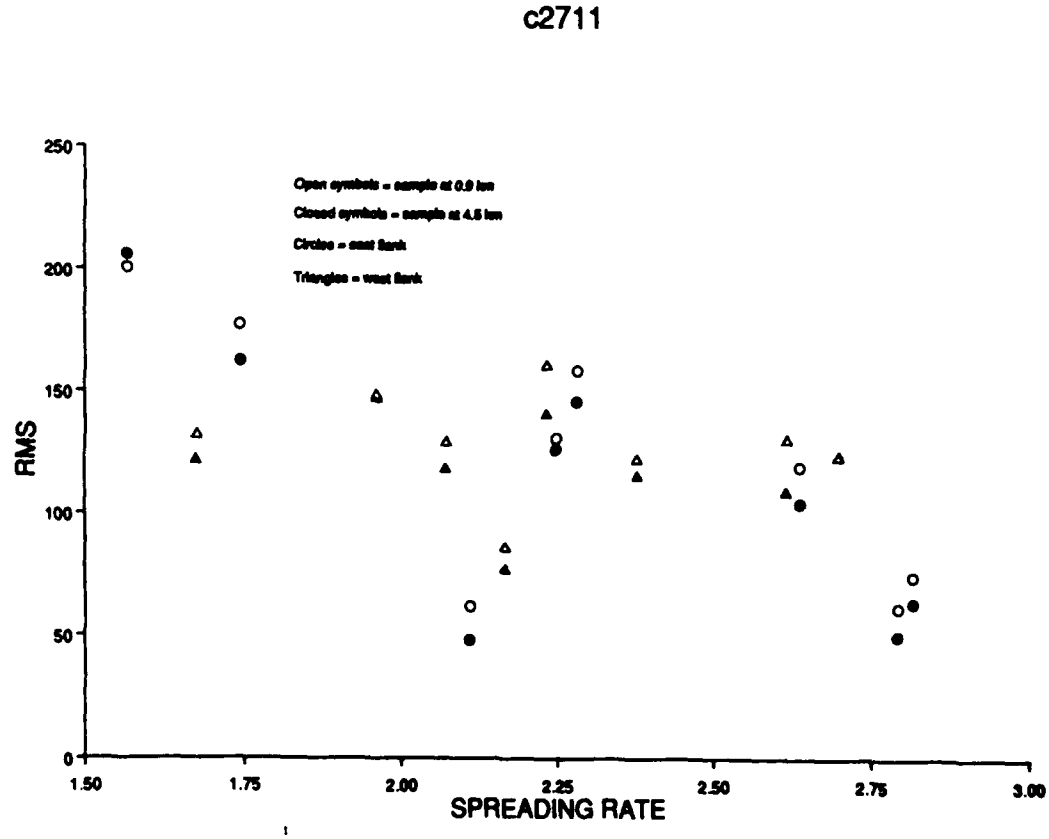

Figure 2B

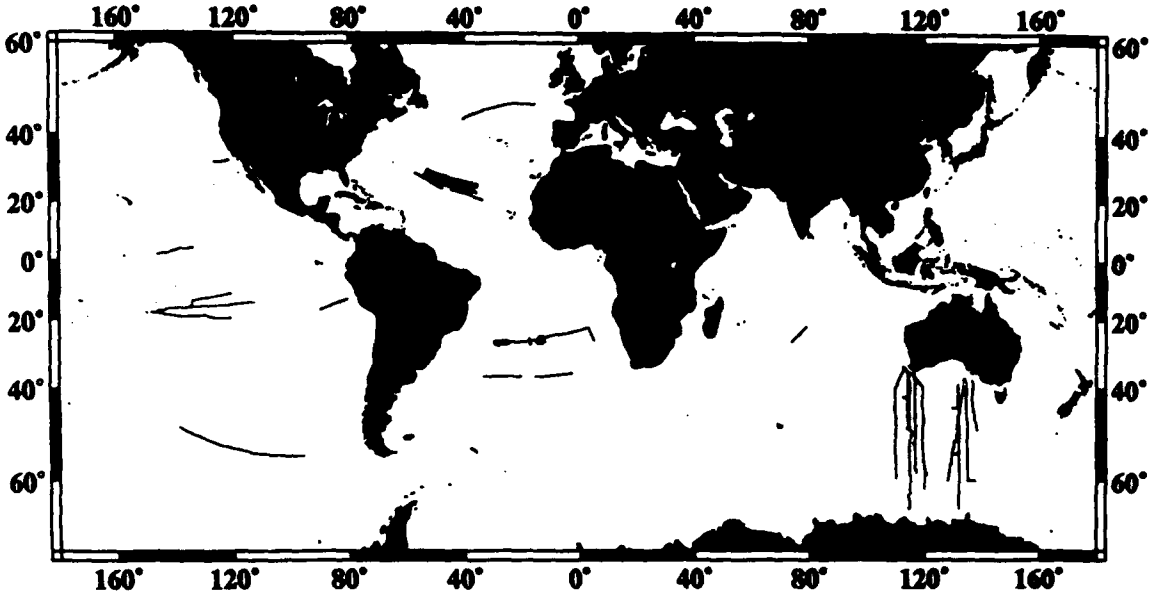

Figure 3A

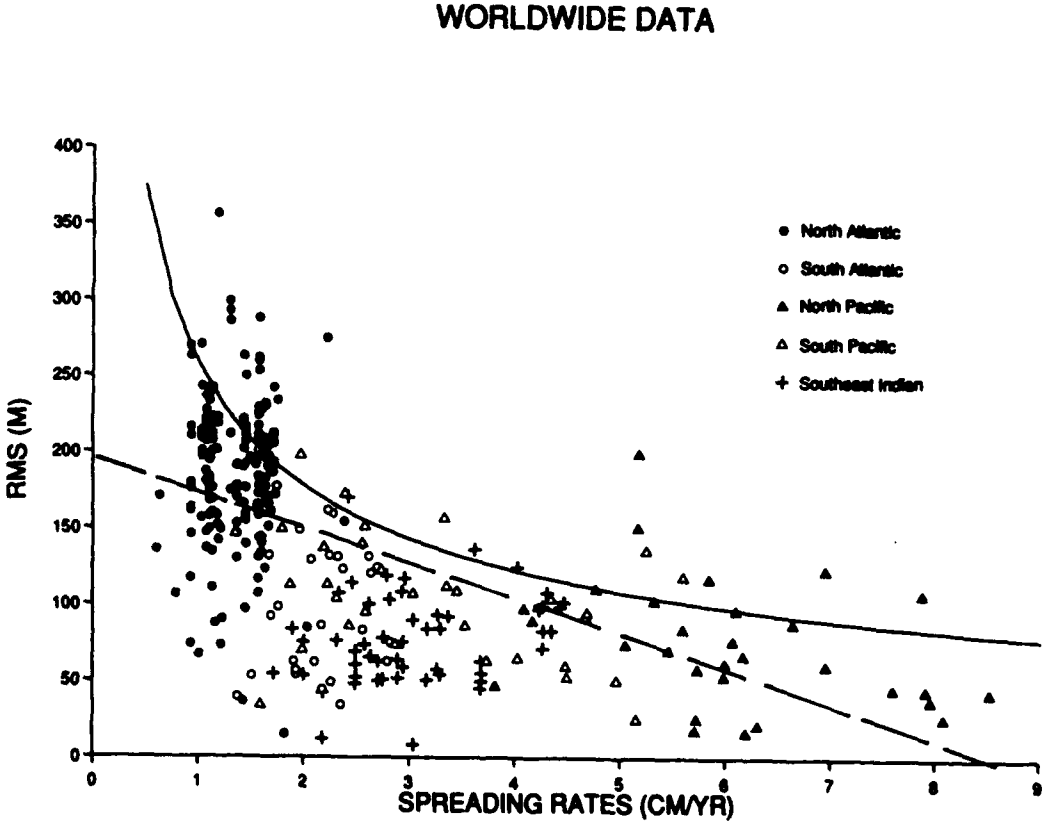

Figure 3B

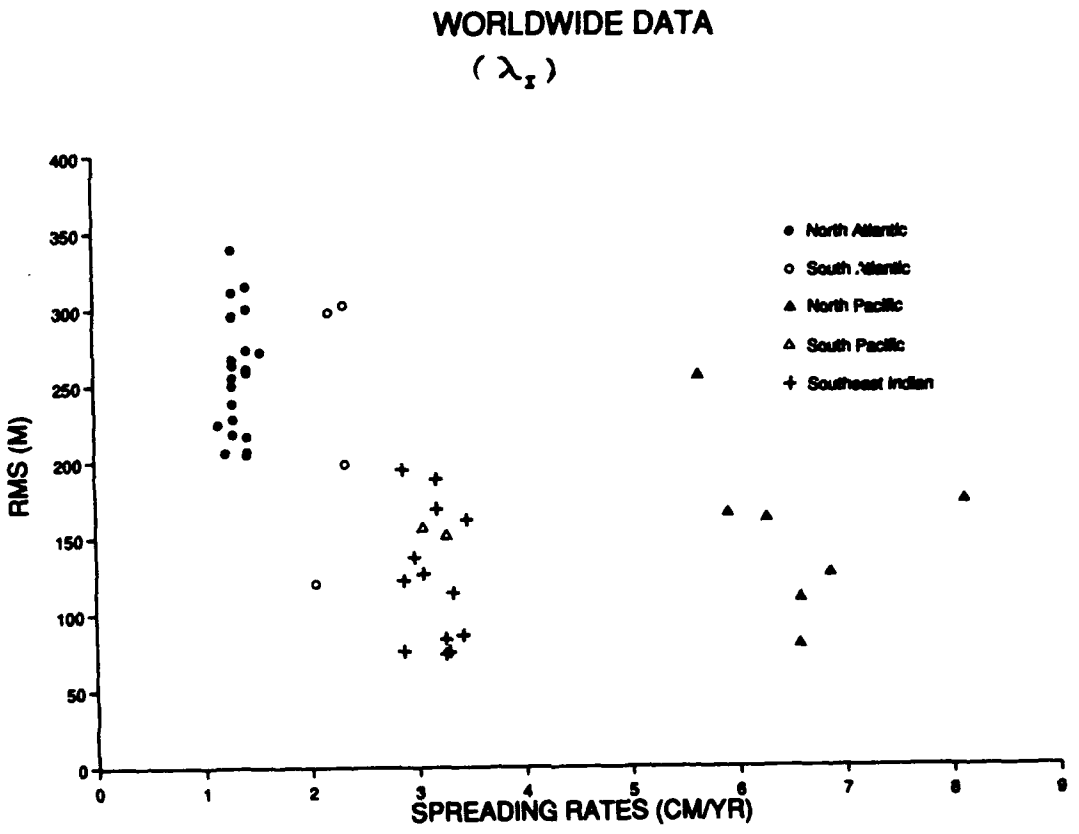
WORLDWIDE DATA
(λ_I)
RMS (M)
SPREADING RATES (CM/YR)
North Atlantic
South Atlantic
North Pacific
South Pacific
Southeast Indian
400
350
300
250
200
150
100
50
0
0
1
2
3
4
5
6
7
8
9

Figure 3C

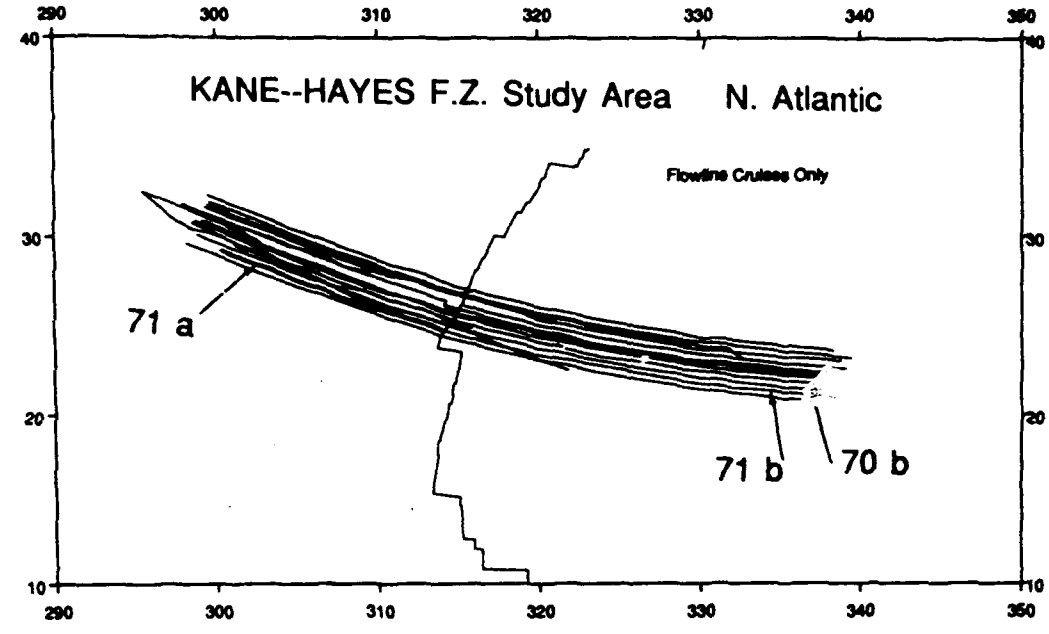

Figure 4A

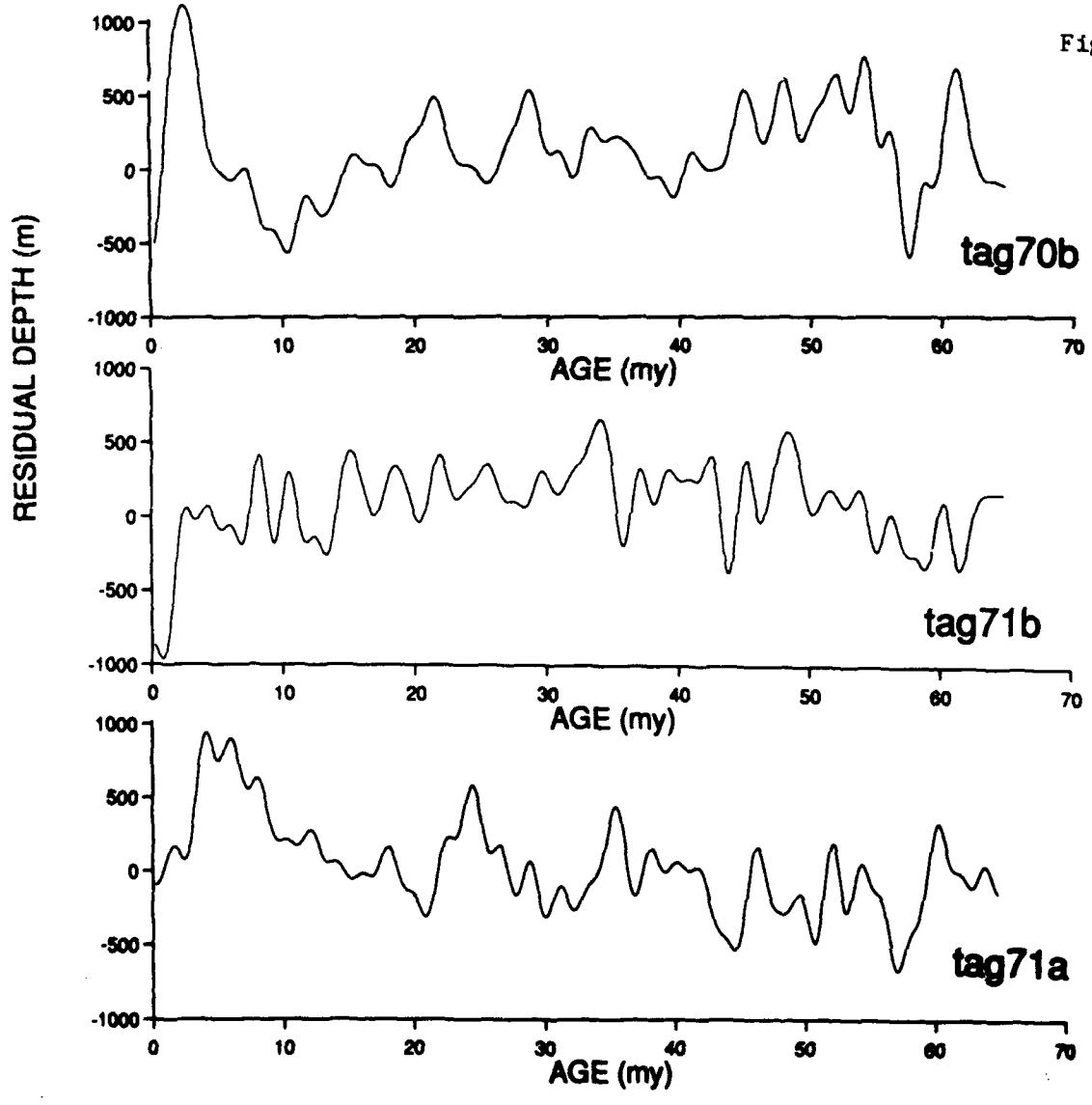

Figure 4B

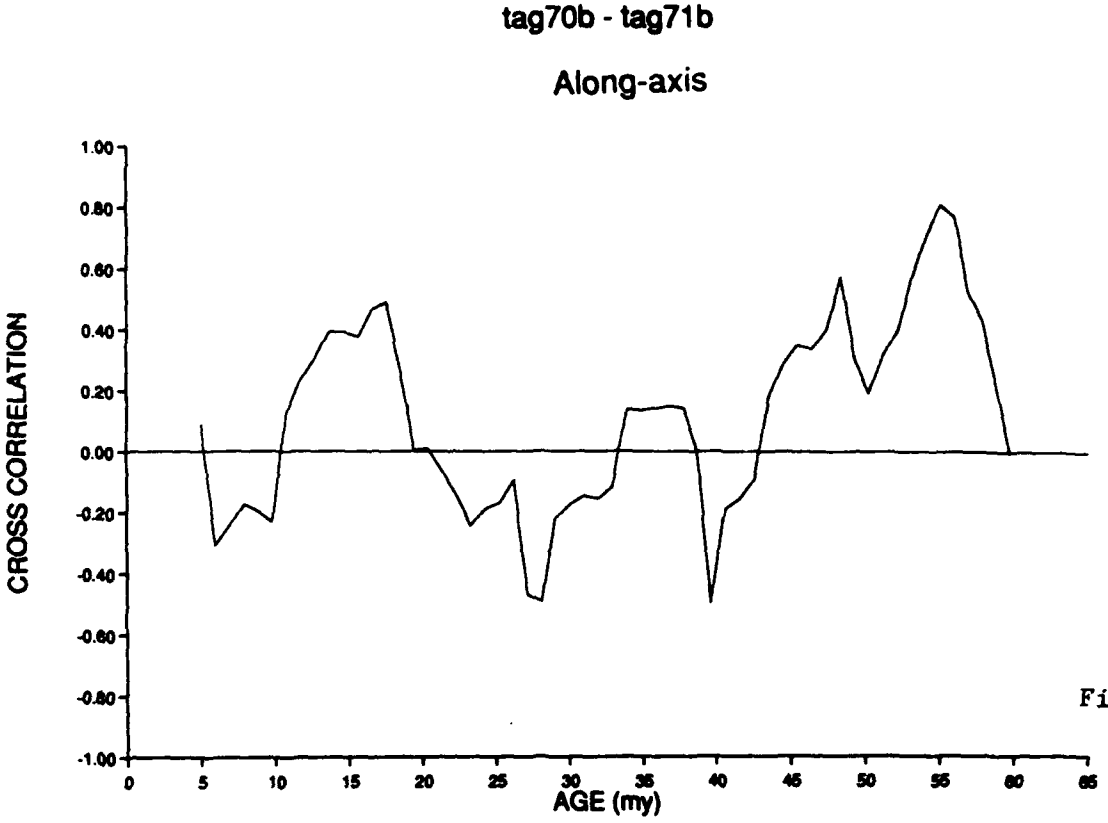

Figure 4C

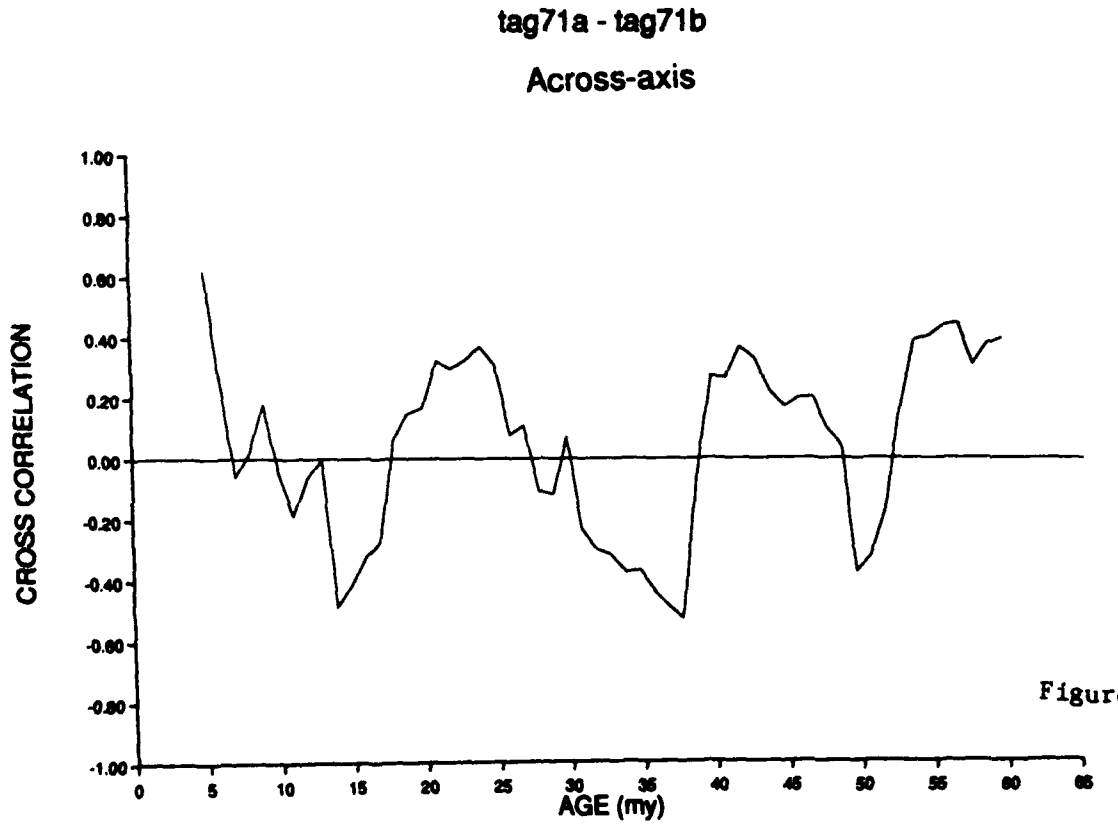

Figure 4D